

Mol #50963

## **Mutagenic Mapping Suggests a Novel Binding Mode for Selective Agonists of M<sub>1</sub> Muscarinic Acetylcholine Receptors.**

**Guillaume Lebon<sup>1</sup>, Christopher J. Langmead, Ben G. Tehan and Edward C. Hulme,**

Division of Physical Biochemistry, MRC National Institute for Medical Research, Mill Hill,  
London NW7 1AA, United Kingdom (E.C.H., G.L.) and GlaxoSmithKline, New Frontiers  
Science Park, Harlow, Essex CM19 5AW, United Kingdom (C.J.L, B.G.T).

Mol #50963

**Running Title:**

Mapping Selective Muscarinic Agonists

Corresponding author:

Dr. E.C. Hulme, Division of Physical Biochemistry, MRC National Institute for Medical Research, Mill Hill, London NW7 1AA, U.K., Tel: (44)208-816-2057; Fax (44)208-906-4477;  
Email: ehulme@nimr.mrc.ac.uk

Text pages: 36;

Tables: 3;

Figures: 6;

References: 33;

Abstract: 248 words;

Introduction: 749 words;

Discussion: 1500 words.

Abbreviations:

NSA, novel selective agonist (AC-42, 77-LH-28-1, NDMC); mAChR, muscarinic acetylcholine receptor; ACh, acetylcholine; TM, transmembrane domain; ECL extracellular loop; NMS, (-)-N-methyl scopolamine; QNB, 3-quinuclidinyl benzilate; PhI phosphoinositide; NDMC, N-desmethylclozapine; AC-42, 4-n-butyl-1-[4-(2-methylphenyl)-4-oxo-1-butyl]-piperidine; 77-LH-28-1, 1-[3-(4-butyl-1-piperidinyl)propyl]-3,4-dihydro-2(1H)-quinolinone; PBS, phosphate-buffered saline; SPA, scintillation proximity assay; nH slope factor.

Mol #50963

## ABSTRACT

Point mutations and molecular modelling have been used to study the activation of the M<sub>1</sub> muscarinic acetylcholine receptor (M<sub>1</sub> mAChR ) by the functionally-selective agonists 4-n-butyl-1-[4-(2-methylphenyl)-4-oxo-1-butyl]-piperidine (AC-42), and 1-[3-(4-butyl-1-piperidinyl)propyl]-3,4-dihydro-2(1H)-quinolinone (77-LH-28-1), comparing them to N-desmethylclozapine (NDMC) and ACh. Unlike NDMC and ACh, the activities of AC-42 and 77-LH-28-1 were undiminished by mutations of Tyr404 and Cys407 (transmembrane helix 7), although reduced by mutations of Tyr408. Signalling by AC-42, 77-LH-28-1 and NDMC was reduced by Leu102Ala and abolished by Asp105Glu, suggesting that all three may interact with transmembrane helix 3 at or near the binding site Asp105, to activate the M<sub>1</sub> mAChR. In striking contrast to NDMC and ACh, the affinities of AC-42 and 77-LH-28-1 were increased 100-fold by Trp101Ala , and their signalling activities abolished by Tyr82Ala. Tyr82 and Leu102 contact the indole ring of Trp101 in a structural model of the M<sub>1</sub> mAChR. We suggest the hypothesis that the side-chain of Trp101 undergoes conformational isomerisation, opening a novel binding site for the aromatic side-chain of the AC-42 analogues. This may allow the positively-charged piperidine nitrogen of the ligands to access the neighbouring Asp105 carboxylate to activate signalling, following a vector within the binding site that is distinct from that of acetylcholine. NDMC does not appear to use this mechanism. Subtype-specific differences in the free energy of rotation of the side-chain and indole ring of Trp101 might underlie the M<sub>1</sub>-selectivity of the AC-42 analogues. Trp conformational isomerisation may open up new avenues in selective muscarinic receptor drug design.

Mol #50963

The M<sub>1</sub> muscarinic receptor (mAChR) is an attractive drug target to treat Alzheimer's disease and schizophrenia (Langmead *et al.*, 2008b). The amino acid side-chains that contact acetylcholine are modelled on the inward-facing segments of transmembrane (TM) helices 3, 4, 5, 6 and 7 within the outer leaflet of the lipid bilayer (Hulme *et al.*, 2003). Their conservation between the five receptor subtypes has restricted the discovery of selective agonists.

AC-42 is a novel ligand that activates M<sub>1</sub> mAChRs selectively (Spalding *et al.*, 2002). Activation is little affected by Ala-substitution of the orthosteric binding pocket residues Tyr381 (6.51; Ballesteros and Weinstein, 1995) and Asn382 (6.52), but requires sequences in the N-terminus and TM1, and extracellular loop (ECL) 3 and the outer part of TM7. Thus AC-42 may activate M<sub>1</sub> mAChRs from a distinct "ectopic" site (Spalding *et al.*, 2002). Supporting this, AC-42 can display allosteric interactions with N-methyl scopolamine (NMS) and atropine (Langmead *et al.*, 2006). A study of TM3 showed that activation of M<sub>1</sub> mAChRs by AC-42 analogues was unaffected by Ala-substitution of Tyr106 (3.33) neighbouring the ACh counter-ion Asp105 (3.32), or Ser109 (3.36) one helical turn below, but was inhibited by L102A (3.29) and paradoxically very strongly potentiated by W101A (3.28), one helical turn above (Spalding *et al.*, 2006). The compounds did not activate D105A, but ACh itself is also completely inactive at this mutant.

N-desmethylozapine (NDMC) is a metabolite of the anti-psychotic drug clozapine that has agonist activity at M<sub>1</sub>, M<sub>3</sub> and M<sub>5</sub> but not M<sub>2</sub> and M<sub>4</sub> mAChRs (Davies *et al.*, 2005). Unlike ACh, its activity is potentiated by Y381A (Sur *et al.*, 2003), and preserved by Y106A and S109A

Mol #50963

(Spalding *et al.*, 2006), Unlike AC-42 its potency is not enhanced by W101A, suggesting a variant mode of interaction.

TM2 does not participate in binding ACh or NMS (Bee and Hulme, 2007). However, in a range of receptors, TM2, TM3 and TM7 define a subsidiary binding pocket (Leonardi *et al.*, 2004; de Mendonca *et al.*, 2005; Flanagan *et al.*, 2000; Stitham *et al.*, 2003; Jensen *et al.*, 2007). An aromatic cluster between TM2 and TM3 may contribute to the activation of CCR5 by chemokines (Govaerts *et al.*, 2003) and be a determinant of D<sub>2</sub> vs D<sub>4</sub> receptor selectivity (Simpson *et al.*, 1999; Schetz *et al.*, 2000).

Optimised molecular models of the M<sub>1</sub> mAChR (Goodwin *et al.*, 2007) also show a well-packed microdomain enriched in hydrophobic and aromatic amino acids at the top of TM2, TM3 and TM7. The side-chains of Tyr82 (2.61) and Leu102 may be close to the ring of Trp101, while Met79 (2.58) may help to buttress the ring of Tyr408 (7.43) (Bee and Hulme, 2007). Notably, the hydroxyl group of the homolog of Tyr408 may be hydrogen bonded to the binding site Asp as in the crystal structure of the  $\beta$ 2 adrenergic receptor (Cherezov *et al.*, 2007).

TM3 and TM7 define the frontier between the major and subsidiary pockets. Asp105 (Lu and Hulme, 1999), Tyr404 (7.39) and Cys407 (7.42) (Lu *et al.*, 2001) lie within the major orthosteric pocket. Met79 and Tyr82 are better classified as belonging to the subsidiary pocket. This is consistent with the limited effects of the Y82A and M79A mutations on ACh-mediated activation of the M<sub>1</sub> mAChR (Lee *et al.*, 1996; Bee and Hulme, 2007). Trp101 and Leu102 are in the “second shell” of the ACh binding site (Lu and Hulme, 1999). However, certain residues, particularly Tyr408, may be at the interface of the two pockets and able to contribute to both.

Mol #50963

In this study, we have investigated the effect of mutations of these residues on binding and activation of M<sub>1</sub> mAChRs by AC-42, its analogue 77-LH-28-1 (Langmead *et al.*, 2008a) and NDMC (for convenience, collectively designated novel selective agonists, NSAs) comparing them to ACh. We have included a control residue, Leu100, believed to face towards the lipid bilayer. To evaluate the importance of the binding site Asp, we have used the D105E mutant. This strongly reduces the potency of activation of the M<sub>1</sub> mAChR by ACh without abolishing the signalling response (Page *et al.*, 1995), providing a more discriminating probe than D105A. The results suggest that the AC-42 analogues may activate the M<sub>1</sub> mAChR by a novel conformational trapping mechanism, whereby a moiety of the ligand replaces the indole ring of Trp101 within the structure of the receptor after rotation of the side-chain. This may allow the presentation of the charged piperidine headgroup of the ligands to the Asp105 counter-ion following a vector distinct from that of ACh.

## Materials and Methods.

**Materials.** (-)-N-[<sup>3</sup>H]methylscopolamine (82, 84 Ci/mmol), (-)-[<sup>3</sup>H]quinuclidinyl benzilate (42Ci/mmol) and myo-D-[<sup>3</sup>H]inositol (80 Ci/mmol) were purchased from GE Healthcare (Chalfont St. Giles, Buckinghamshire, UK). Unlabelled ligands were from Sigma-Aldrich (Gillingham, UK). AC-42 and 77-LH-28-1 were synthesised as described (Langmead *et al.*, 2006; Langmead *et al.*, 2008a). Stock solutions (10<sup>-2</sup> M) were prepared in DMSO and stored at -20 °C. Ligand dilutions were prepared in DMSO.

Mol #50963

**DNA and expression.** With the exception of Y82A, the rat M<sub>1</sub> mutant receptors used in this work have been described previously (Bee and Hulme, 2007; Lu and Hulme, 1999; Lu *et al.*, 2001; Page *et al.*, 1995). They were cloned in the pCD expression vector and were transiently expressed in COS-7 cells grown in MEM  $\alpha$  media supplemented with 10% New Born Calf Serum and 1% Glutamate, at 37°C in 5% CO<sub>2</sub>. Around 2 x10<sup>7</sup> cells (1 cuvette) were transfected by electroporation with 15  $\mu$ g of DNA using a BioRad Gene Pulser (260 volts, 960 microfarads). The transfected cells were re-suspended in 30 ml of warm supplemented media and plated into 3 dishes (10 ml;  $\approx$  6.5 x 10<sup>6</sup> cells/ plate) for the binding experiments and into 96 well plates (200  $\mu$ l per well;  $\approx$  1.5x 10<sup>5</sup> cells/well) for the phosphoinositide turnover assays. 24 h after the transfection cells were washed twice in warmed phosphate-buffered saline (PBS) and new MEM  $\alpha$  media added. When necessary, the media was supplemented with atropine (10<sup>-6</sup>M) to rescue the low expressing mutant receptors (M79A, Y404A, Y408A) as described previously (Bee and Hulme, 2007; Lu *et al.*, 2001). Y82A was constructed by the QuickChange (Stratagene) procedure, and verified by di-deoxy nucleotide sequencing.

**Cell membrane preparation.** Membrane preparations were made 72 h after transient transfection. The COS-7 transfected cells were washed twice with PBS. Cells were harvested in 20 mM Na-HEPES, 10 mM EDTA, pH 7.5, 4°C (1 ml per dish) and homogenised by using a mechanical glass homogeniser. Membranes were pelleted by centrifugation, 30 min at 30,000 g and were re-suspended in storage buffer, 20 mM Na-HEPES, 1mM EDTA, pH 7.5 and then homogenised using a Polytron PT3100 (twice 15 secs, 12000 rpm). 1ml aliquots were snap-frozen on dry ice and stored at -80°C.

Mol #50963

**Radioligand binding assays.** Binding experiments were carried out in 96 well plates (2 ml deep, polystyrene plates) using three different concentrations of [<sup>3</sup>H]NMS equal, where possible, to 0.1 x , 2 x and 10 x the K<sub>d</sub> of [<sup>3</sup>H]NMS for the particular mutant. Each agonist concentration was performed in quadruplicate. Membrane preparations were spun at 14000 rpm (17000 g) then re-suspended in binding buffer (20 mM Na-HEPES, 0.1 M NaCl, 1 mM MgCl<sub>2</sub>, pH 7.5). The membrane suspension was homogenised with the polytron PT3 100 (15 secs, 12000 rpm). 10 µl of diluted compounds in DMSO, 10 µl [<sup>3</sup>H] NMS diluted in binding buffer were mixed with 980 µl of membrane preparation (7 – 30 µg membrane protein/ml), the plates were covered with a plastic seal and incubated 2 hours (4 hours for the W101A mutant) at 30°C. Binding was stopped by filtration on to Wallac 96-Printed GF/B filtermats using a TOMTEC Harvester 96, MACH III M. The filtermats were washed three times with 3 ml of cold ddH<sub>2</sub>O. The filters were dried at 55 °C for approximately 1hour. A solid Melt-on Scintillator Sheet was melted on to the filtermat containing the harvested membranes. Radioactivity was counted on a normalised, calibrated 1450 Microbeta Trilux counter (5 min per sample). The expression level of the wild-type receptor was 2.92 ± 0.80 pmol/mg membrane protein (mean ± SD). This corresponds to ~ 2 x 10<sup>5</sup> [<sup>3</sup>H]NMS binding sites per cell (Bee and Hulme, 2007). Expression levels of the mutants (% wild-type) were as follows: M79A, 96%; Y82A, 36%; L100A, 102%; L102A, 76%; W101A, 47%; D105E, 46%; Y404A, 109%; Y404F, 125%; C407A, 107%; Y408A, 162%; Y408F, 99%.

**Phosphoinositide functional response.** Measurement of G-protein-coupled receptor activation was carried out using a scintillation proximity assay (SPA) of inositol phosphates in cell extracts (Brandish *et al.*, 2003) with some modifications. Transfected cells were grown in 96



Mol #50963

well plates at 37°C, 5% CO<sub>2</sub>. After 24 hours, the cells were washed twice in warm PBS and labelled with 2.5 µCi/ml *myo*-D-[<sup>3</sup>H]inositol in medium for 48 hours. After 48 hours, *myo*-D-[<sup>3</sup>H]inositol was removed, the cells washed twice in warm PBS and once in Krebs solution containing 10 mM LiCl and finally incubated for 30 min in Krebs/Li, 37°C, 5% CO<sub>2</sub>. Cells were then incubated with 100 µl of agonist (diluted in Krebs/Li solution to the final concentration required) for 1 hour at 37°C, 5% CO<sub>2</sub>. The reaction was terminated by the removal of the agonist dilution and the addition of 200 µl of 0.1 M formic acid. The cell solubilisation was allowed to continue for 1 hour at room temperature after which 20 µl samples of the lysates were mixed with 80 µl of RNA binding yttrium silicate SPA beads (12.5 mg/ml) in 96 well isoplates. Plates were agitated for 1 hour and then the beads left to settle for 2 hours protected from the light. The accumulation of negatively charged [<sup>3</sup>H] inositol phosphates was determined using a 1450 Microbeta Trilux counter (5 min per sample). In each experiment, atropine (10<sup>-6</sup> M) was added to one triplicate set of assays to control for atropine-sensitive ACh-independent constitutive activity. This was maximally 8.5 % for the wild-type receptor.

**Data analysis.** Binding curves and phosphoinositide (PhI) dose response curves were fitted using SigmaPlot (version 10). Binding curves for [<sup>3</sup>H]NMS in the presence of agonists were fitted to an allosteric ternary complex model of binding in which the apparent affinity constant for the radioligand is given by the following expression:

$$K_{app} = K_L \cdot (1 + \alpha (K_A \cdot [A])^{nH}) / (1 + K_I \cdot [I] + (K_A \cdot [A])^{nH}) \dots \dots \dots (1)$$

This analysis yields an affinity constant (-log M) for NMS (K<sub>L</sub>), for the compounds (K<sub>A</sub>), an expression level value of the receptor (R<sub>T</sub>) and in the case of mutants displaying allosteric behaviour, a cooperativity factor value (α) and a slope factor (nH). Non-specific binding was

Mol #50963

determined with  $10^{-6}$  M unlabelled NMS (designated [I]). The equations were written to compensate for any radioligand depletion (less than 10 %). The three data sets for a particular combination of mutant and unlabelled ligand, acquired using [ $^3$ H]NMS concentrations equivalent to 0.1 x, 2 x and 10 x the  $K_d$  value for the particular mutant wherever possible, were first analysed simultaneously providing estimates of the affinity constants and the cooperativity factor in a logarithmic form. Fits were compared using the F-statistic. The cooperativity factor is quoted only when the increase in the goodness-of-fit compared to the competitive model ( $\alpha=0$ ) was significant at the 1 % level. The three data sets for each compound were then re-analysed as independent experiments using the Hill equation. The  $pIC_{50}$  values were corrected for the Cheng-Prusoff shift, using the mean affinity constant for [ $^3$ H]NMS from 5 independent measurements, to calculate individual  $pK_d$  values. These were used in statistical analysis by 1-way ANOVA as detailed below. The  $pK_d$  values from the two methods of analysis were not significantly different (mean difference =  $0.044 \pm 0.044$ , mean  $\pm$  SD) except in the case of AC-42 at Y82A ( $pK_d$ , allosteric ternary complex model = 6.25;  $pK_d$  Hill analysis = 5.75). This gave the highest cooperativity factor (0.12) of any ligand-mutant combination, rendering Hill analysis inappropriate. Thus, the all of the values given are from global fits to the allosteric ternary complex model. Values are tabulated as  $pK_d \pm$  SEM.

PhI dose-response curves were fitted to a four-parameter logistic function, yielding  $E_{Max}$ ,  $E_{Basal}$  and  $pEC_{50}$  values for each NSA at the particular mutant under study. Slope factors were close to 1.0.  $E_{Max}$  values for the NSAs, corrected for basal signaling, were expressed relative to the corresponding values for ACh in the same experiment as follows  $E_{MaxN} = (E_{MaxNSA} - E_{Basal}) / (E_{MaxACh} - E_{Basal})$ .  $E_{Basal}$  was the measurement obtained in the presence of atropine,

Mol #50963

except in the case of L102A, D105E and Y404A where the values were not different.  $pEC_{50}$  and  $E_{MaxN}$  values are tabulated. The values are mean  $\pm$  SEM of 3-4 separate measurements.

**Statistical analysis.** One-way ANOVA followed by Dunnett's post-hoc test was used to determine the levels of significance of differences between the means.

**Construction of the M<sub>1</sub> mAChR model.** The initial model of the TM domain of human M<sub>1</sub> receptor was constructed by homology with the published high-resolution X-ray crystal structure of the  $\beta$ 2-adrenergic receptor (Cherezov *et al.*, 2007). Alignment between the M<sub>1</sub> sequence and  $\beta$ 2 was based on the "classic" motifs found in each TM region, the asparagine in TM1, the aspartate in TM2, the "DRY" motif of TM3, the tryptophan in TM4, and the conserved prolines in TM5, TM6 and TM7. These alignments were used, with the standard homology modelling tools in the Quanta program to construct the seven helical bundle domain of M<sub>1</sub>. The extracellular loop regions were subsequently added using a procedure developed within GlaxoSmithKline, which makes use of a combined distance geometry sampling and molecular dynamics simulation (Blaney *et al.*, 2001) The side-chains of this model were then refined using the Karplus standard rotamer library (Dunbrack and Karplus, 1993). The final model was optimised fully (500 steps of Steepest Descent (SD) followed by 5000 steps of Adopted Basis Newton Raphson (ABNR)) with the CHARMM force field (Brooks *et al.*, 1983) using helical distance constraints between the *ith* and *i+4th* residues (except proline) within a range of 1.8Å-2.5Å, to maintain the backbone hydrogen bonds of the helix bundle. A distance-dependent dielectric was used by selecting the CHARMM keyword RDIE, thought to be more appropriate when relaxing a structure.

Mol #50963

A variant of the model was constructed in which the  $\chi_1$  angle of Trp101 prior to the final minimisation step was manually adjusted from trans to gauche<sup>+</sup> ( $\chi_1 = -60^\circ$ ). This enabled the energy difference between the two different states of the receptor to be calculated. The calculated energy difference is given in kcal/mol.

**Ligand docking studies.** Ligand molecules were built and optimized within Spartan (SPARTAN SGI, version 5.1.3, Wavefunction, Inc., Irvine, CA) using an AM1 Hamiltonian. The atom-centered charges for the ligands, used in the docking studies, were natural atomic orbital charges calculated at the Hartree-Fock level within Spartan, using a 6-31G\* basis set.

Ligands were docked into the receptor model manually using a variety of low energy starting conformations. The starting conformation of the Trp101 side-chain was gauche<sup>+</sup> ( $\chi_1 = -60^\circ$ ). Adjustments of the receptor protein side-chains were made where necessary, always ensuring that these side-chains were only in allowed rotameric states (Dunbrack and Karplus, 1993). Once again, full optimisation of the receptor-ligand complexes was performed using CHARMM, the only constraints used being those which maintained the hydrogen bonding pattern of the helical bundle and the charge-charge interaction between the basic nitrogen of our ligand species and the acidic head-group of Asp105 on TM3. This procedure allows full relaxation of both the ligand and the whole protein, something which is not possible with automated docking procedures.

After energy minimisation, the interaction energies of the ligand 77-LH-28-1 and the indole component of the Trp101 side-chain with the nearest- neighbour residues Tyr82 and Leu102 were calculated by energy deconvolution. These represent the sum of the electrostatic and the Van der Waals energy contributions from all of the atoms in these two residues that interact either with

Mol #50963

the ligand, or with the indole moiety of the Trp101 side-chain. The force field used was CHARMM. Energies are given in kcal/mol. A value for the universal gas constant of 1.986 cal/°/mol was used to calculate the free energies corresponding to changes in the ligand affinity constants, measured at the assay temperature of 303 °K.

## Results.

**Ligand binding studies.** The binding of the unlabelled ligands to wild-type and mutant M<sub>1</sub> mAChRs was investigated by measuring inhibition of the binding of three concentrations of [<sup>3</sup>H]NMS, equal (where possible) to 0.1 x K<sub>d</sub>, 2 x K<sub>d</sub> and 10 x the K<sub>d</sub> value of the radioligand for the particular mutant. The inhibition curves were analysed simultaneously using an allosteric ternary complex model of binding. This allowed three parameters to be estimated for each ligand (a) the affinity of the ligand for the unoccupied receptor, measured by its pK<sub>d</sub>; (b) its cooperativity with the tracer ligand NMS, measured by the cooperativity factor  $\alpha$  and (c) a slope factor, usually about 0.9. In addition, the experimental design provided a measure of the expression level of the mutant receptor, and a 3-point estimate of its affinity for [<sup>3</sup>H]NMS, providing a useful set of data for comparison with previous studies in the laboratory. The mutants were expressed at levels ranging from 36% to 162 % of the wild-type (Materials and Methods). The pK<sub>d</sub> value and slope factor for ACh binding to the wild-type receptor were 4.97 ± 0.07 and 0.87 ± 0.03 respectively. These are in good agreement with published values, as are the affinity constants of NMS for the mutant receptors (Table 1) (Bee and Hulme, 2007; Lu *et al.*, 2001; Lu and Hulme, 1999; Page *et al.*, 1995).

The pK<sub>d</sub> values for binding of the NSAs (the structures are shown in Fig. 1a) to the wild-type M<sub>1</sub> mAChR were 6.14 ± 0.12 (AC-42), 6.56 ± 0.08 (77-LH-28-1)) and 7.41 ± 0.05 (NDMC;

Mol #50963

Table 1). The values for AC-42 and NDMC agree well with published estimates (Sur *et al.*, 2003; Spalding *et al.*, 2006; Spalding *et al.*, 2002; Langmead *et al.*, 2006). All of the ligands behaved competitively with respect to [<sup>3</sup>H]-NMS in equilibrium binding assays with the wild-type receptor, giving full inhibition of radioligand binding. A representative experiment is shown in Fig. 2a. This illustrates the good fit obtained to a competitive model of interaction between 77-LH-28-1 and [<sup>3</sup>H]NMS. Under our experimental conditions, this implies a cooperativity factor  $\alpha < 0.01$ .

The affinities of the NSAs (Table 1) showed two different patterns of response to the mutations (the distribution of the mutants is shown in Fig. 1b). The changes in the pK<sub>d</sub> values are plotted in Fig. 3, where they are compared to the values for NMS. AC-42 and 77-LH-28-1 exhibited a similar pattern. They showed 5-8-fold reductions in affinity for the M79A and Y408F mutants. As described previously for AC-42 (Spalding *et al.*, 2006), they displayed 70- and 275-fold increases in affinity for the W101A mutant (Table 1). Representative data are given in Fig 2b. For 77-LH-28-1, the fit of the allosteric ternary complex model to the data was significantly improved ( $P < 0.01$ ) by a value for the cooperativity factor slightly greater than zero ( $\alpha = 0.018$ ), although the binding of AC-42 and [<sup>3</sup>H]NMS to the W101A mutant remained apparently competitive ( $\alpha < 0.01$ ). There were no affinity changes exceeding 2.5-fold in response to any of the other mutations, although an increase in affinity of AC-42 for the L102A mutant was statistically significant.

Interestingly, Ala mutation of Tyr82 caused the emergence of clear allosteric (non-competitive) binding behaviour for both ligands with respect to [<sup>3</sup>H] NMS with cooperativity factors of 0.12 for AC-42 and 0.046 for 77-LH-28-1 (Table 1; Fig. 2c). This implies that the removal of the Tyr82 side-chain allows both of the interacting ligands to bind simultaneously to

Mol #50963

the mutant receptor to form a ternary complex. The cooperativity factor is the ratio of the affinity constants of the unlabelled ligand for the NMS-occupied and unoccupied receptor. Thus, we were also able to estimate the affinity of the ligand for the NMS-occupied receptor. Upper limits for the affinity constants at the wild type NMS-occupied receptor were obtained by assuming that, in the case of competitive behaviour, the cooperativity factor  $\alpha$  must be  $\leq 0.01$ .  $pK_d$  values of 5.2-5.3 for AC-42 and 77-LH-28-1 were obtained at the NMS-occupied Y82A mutant, but these values must be  $\leq 4.1$ , 4.6, respectively, at the NMS-occupied WT receptor, representing increases in affinity of 5-10-fold. There was also evidence that the L102A mutation elicited allosteric binding behaviour with AC-42 (Table 1), and possibly with 77-LH-28-1, although this was at the limit of detectability ( $\alpha = 0.01$ ).

NDMC showed a different pattern of behaviour to AC-42 and 77-LH-28-1, with small reductions in affinity at W101A, L102A, D105E Y404A and C407A compared to the wild-type receptor, resembling, in this respect, an attenuated version of NMS or ACh (Table 1; Fig. 3). However, unlike NMS and the other compounds, the affinity of NDMC was slightly (2.75-fold) increased by the Y408A mutation. The affinity of NDMC was not altered by the W101A mutation. There was evidence of allosteric interactions between NDMC and NMS in binding to the Y404A mutant ( $\alpha = 0.046$ ).

**Phosphoinositide assay.** The functional responses of mutants to the binding of ACh and the NSAs have been studied by measuring total phosphoinositide breakdown, using a scintillation proximity assay to quantitate the accumulation of labelled phosphoinositides. Analysis of the

Mol #50963

dose-response curve for each agonist at each mutant has yielded estimates of (a) the potency, measured by the pEC<sub>50</sub> value and (b) the maximum response (E<sub>MaxN</sub>) relative to that evoked by ACh at the same mutant. The results are summarised in Table 2.

For ACh, the present study is in good agreement with previously published work (Bee and Hulme, 2007; Goodwin *et al.*, 2007 ;Lu *et al.*, 2001; Lu and Hulme, 1999; Page *et al.*, 1995). ACh stimulated all of the mutants with E<sub>Max</sub> values between 65 % (Y404A) and 94 % (C407A) of the value obtained for the wild-type receptor (values not significantly different to wild-type receptor, P>0.1). The ratio of the ACh-induced maximum signal to the basal ACh-independent signal ranged from 4.7 to 9-fold. The mean value for the wild-type receptor was 5.2. The pEC<sub>50</sub> of ACh at the wild-type receptor was 6.92 ± 0.04 (Table 2) in excellent agreement with previous values. The potency of ACh is reduced by almost 1000-fold by the D105E mutation (Page *et al.*, 1995); this was reproduced (524-fold reduction) in the present study, which also confirmed large reductions in potency for the mutations of Trp101, Leu102, Tyr404, Cys407 and Tyr408 (Table 2).

The NSAs all stimulated the PhI response at the wild-type receptor (Fig. 4a, Table 2). AC-42 and 77-LH-28-1 acted as partial agonists with maximum responses at levels of 64 and 74 % of the ACh-induced maximum response respectively. 10<sup>-5</sup> M NDMC evoked 52% of the ACh-induced maximum PhI response of the wild-type receptor, but the highest concentration tested (10<sup>-4</sup> M) showed a reduced signal, possibly indicating a non-specific toxic effect on the cells (data not shown).

The NSAs evoked maximum responses not significantly different to the wild-type values or the internal ACh controls (Table 2) from most of the mutant receptors. Four mutants showed



Mol #50963

strongly reduced signalling. These were D105E (Fig.4b) for which receptor signalling by all three compounds was completely abolished; Y82A, at which only NDMC evoked a quantifiable response (Fig. 4c); L102A whose maximum response to all three of the NSAs was strongly reduced (Fig. 4d) and Y408A/F, where the AC-42-induced response appeared to be more selectively reduced to less than 50 % of the wild-type value (Fig. 4e). It is interesting that the AC-42 analogues evoked a maximum response comparable to that of ACh from the C407A mutant. In contrast, the maximum response to NDMC was diminished, as was also the case for the Y404F mutant (Table 2).

The relative potencies of AC-42 ( $pEC_{50} = 5.79 \pm 0.03$ ) and 77-LH-28-1 ( $pEC_{50} = 6.68 \pm 0.08$ ) at the wild-type  $M_1$  mAChR were consistent with published values, although the absolute values were 3-4-fold lower, perhaps reflecting our use of COS-7 rather than CHO cells (Spalding *et al.*, 2002; Langmead *et al.*, 2008a). Particular mutations produced large changes in signalling potency (Table 2), best quantified with the more efficacious compound 77-LH-28-1. Consistent with previous reports (Spalding *et al.*, 2006), there was a 100-fold increase in potency for W101A (Fig. 4f), and a 20-fold decrease for L102A (Fig. 4d). In contrast to ACh, the potencies of AC-42 and 77-LH-28-1 were diminished 3-fold by the mutation M79A. Mutations of Tyr408, that diminished the maximum signal, also decreased the potencies of these compounds by up to 25-fold (Fig. 4e), as seen for ACh. In contrast, mutations of Cys407 and Tyr404, while strongly inhibitory to ACh signalling (Lu *et al.*, 2001), preserved or even slightly enhanced signalling by AC-42 and 77-LH-28-1.

For NDMC, the potency at the wild type receptor ( $pEC_{50} = 6.42 \pm 0.05$ ) was in reasonable agreement with literature reports (Spalding *et al.*, 2006; Sur *et al.*, 2003). Nevertheless, the

Mol #50963

potency estimates at each mutant are less reliable because of the bell-shaped concentration-response curves produced by this compound. There was an apparent 3-fold increase in potency ( $P < 0.05$ ) attributable to the Y408A mutation, as seen in the binding data (Fig. 3b). The C407A mutation showed 4-fold reduced potency ( $P < 0.05$ ) for NDMC. With the exceptions of L102A and D105E, no strong effects of the remaining mutations on the potency and signalling efficacy of NDMC were observed.

**Molecular modelling and energy calculations.** The W101A mutation strongly increased the affinity and potency of AC-42 and 77-LH-28-1. In contrast, the Y82A and L102A mutations decreased or abolished signalling by these compounds. These three residues are clustered, both in an optimised molecular model of the  $M_1$  mAChR based on the structure of rhodopsin (Goodwin *et al.*, 2007; not shown) and in an energy-minimised homology model of the  $M_1$  mAChR built on the structure of the  $\beta_2$  adrenergic receptor (Cherezov *et al.*, 2007; Materials and Methods). In the latter model, the indole ring of Trp101, which is in a trans conformation ( $\chi_1 = 167.7^\circ$  after energy minimisation), forms a stacking interaction with the side-chain of Leu102, and an edge-to-face contact with the ring of Tyr82 (Fig. 5a). Energy deconvolution calculations suggested that both contacts involve favourable steric interactions in the range 2.2 – 2.8 kcal/mol (Table 3). Preliminary calculations suggest that other neighbouring residues, such as Trp91 (ECL1), make a smaller contribution (not shown).

The large increases in the affinities of AC-42 (72-fold) and 77-LH-28-1 (275-fold) caused by the W101A mutation suggested that the indole ring of Trp101 may directly obstruct the binding of these ligands. We carried out energy calculations to explore the possibility that the side-chain of 77-LH-28-1 might be capable of replacing the Trp101 indole ring, providing an

Mol #50963

anchor point for the side-chain of the ligand. In the wild-type receptor, though not in the W101A mutant, this requires the preliminary conformational isomerisation of the Trp101 side chain. Manual adjustment of the  $\chi_1$  angle of Trp101 from a trans to a gauche<sup>+</sup> conformation before the final minimisation step (Materials and Methods) increased the calculated overall free energy of the receptor structure by 3.4-3.5 kcal/mol. This unfavourable free energy change is close to the 3.38 kcal/mol calculated from the increased affinity of 77-LH-28-1 binding resulting from the W101A mutation.

Fig. 5b shows 77-LH-28-1 docked into the pocket created by the conformational isomerisation of the Trp101 side-chain, after energy minimisation (Materials and Methods). The view is from outside the helix bundle. The final  $\chi_1$  angle for Trp101 was  $-66^\circ$ . The dihydroquinolinone ring of the selective agonist is complexed between the aromatic ring of Tyr82 and the side-chain of Leu102, consistent with the positioning of the positively charged piperidine nitrogen close to the carboxylate group of Asp105 and the hydroxyl group of Tyr408. Met79 supports the ring of Tyr408, as proposed previously (Bee and Hulme, 2007). Packing interactions of the side-chains of Tyr404 and Cys407 may restrict the binding of the bulky alkyl chain of 77-LH-28-1, modelled as extending into the “subsidiary” binding pocket between TM2, TM3 and TM7. A predicted contact between the alkyl side-chain and Ile74 (2.53) is consistent with a significant reduction of the binding affinity of 77-LH-28-1 by the I74A mutation (G. Lebon, unpublished data). AC-42 can be docked in a similar manner (not shown).

Table 3 summarises the interaction energies, calculated by energy deconvolution, between the atoms of 77-LH-28-1 and the contact residues Tyr82 and Leu102. The bulk of the interaction energy is from the interactions of the dihydroquinolinone ring system, with a smaller contribution

Mol #50963

from interactions of the propyl linker with Tyr82; these components are not differentiated in Table 3. In the case of Leu102, the estimated interaction energy of 2.71 kcal/mol is similar to that of the indole ring of Trp101, so the substitution is broadly energetically neutral. For Tyr82, the computed interaction energy of 5.97 kcal/mol exceeds that computed for the Trp101 indole ring by 3.79 kcal/mol. This is of the right magnitude to overcome the unfavourable effect on the overall free energy of the receptor resulting from the trans-gauche<sup>+</sup> isomerisation of the Trp101 side-chain. It should be noted that these calculations do not take into account factors such as the entropic costs of immobilisation of the ligand side-chain, or desolvation of the ligand, and must therefore be regarded as indicative in nature.

## Discussion

The binding affinity and signalling activity of AC-42, and its more potent analogue 77-LH-28-1 were unaffected or slightly potentiated by mutations of Tyr404 (7.39) and Cys407 (7.42), residues that contribute to the ACh binding pocket (Hulme *et al.*, 2003). These results complement findings in TM3 and TM6 (Spalding *et al.*, 2002; Spalding *et al.*, 2006) and further support a distinct mode of interaction for the AC-42 analogues. In contrast, the binding affinity or maximum signal evoked by NDMC was reduced, suggesting that its binding mode differs from that of the AC-42 analogues (Spalding *et al.*, 2006).

Ala-substitution of Asp105 (3.32) abolishes signalling by AC-42 and NDMC (Spalding *et al.*, 2006). However, this also occurs for ACh (Lu and Hulme, 1999). A less disruptive mutation may be D105E, which repositions the cationic amine counter-ion while preserving its charge. This may also perturb a hydrogen bond to the hydroxyl group of Tyr408 (7.43; Hulme *et al.*,

Mol #50963

1990) homologous to that in the carazolol-ligated  $\beta_2$ -adrenergic receptor (Cherezov *et al.*, 2007). D105E reduces [<sup>3</sup>H]NMS affinity 2-fold and preserves 70% of the maximum signalling capability of ACh, while reducing its potency by 1000-fold (Page *et al.*, 1995).

D105E abolished signalling by AC-42, 77-LH-28-1 and NDMC without altering their binding affinities. Therefore, activation by these compounds depends on the precise position of the counter ion within the receptor binding site. The AC-42 analogues also showed pronounced reductions in binding affinity, signalling potency and efficacy in response to Y408F. As well as abolishing direct interactions of the hydroxyl group with the ligand, this mutation may perturb Asp105 by disrupting the putative stabilising hydrogen bond.

Signalling by the AC-42 analogues and NDMC is preserved by Ala mutation of Ser109 (3.36) but reduced for Asn110 (3.37) and Leu102 (3.29), which are also ACh “second shell” residues (Spalding *et al.*, 2006). We confirmed the effect of L102A on signalling by all three NSAs. However, strong divergence between the AC-42 analogues on the one hand and ACh and NDMC on the other was uncovered in a cluster of residues at the top of TM2 and TM3.

The W101A (3.28) mutation decreases the affinity of ACh by 30-fold (Lu and Hulme, 1999). In contrast, W101A increased the affinities of AC-42 and 77-LH-28-1 by 100-fold or more, into the nanomolar range. NDMC imitated ACh, showing a 4-fold reduction in affinity. These changes were reflected in the signalling potencies rather than the maximum responses of the NSAs, implying that their signalling efficacies remained unchanged. Previously, we have assigned residues whose Ala substitution reduces the binding affinity but not the signalling efficacy of ACh to a ligand-anchor category, helping to ligate the agonist in both the ground and

Mol #50963

the activated states of the receptor (Hulme *et al.*, 2003; Hulme *et al.*, 2007). From this viewpoint, Trp101 behaves as an anti-anchor or bump residue whose indole side-chain directly obstructs the binding of AC-42 and 77-LH-28-1, so that its removal substantially enhances their free energy of binding.

We have investigated two residues at the top of TM2 neighbouring Trp101, namely Met79 (2.58) and Tyr82 (2.61). Confirming previous results (Baig *et al.*, 2005; Bee and Hulme, 2007; Lee *et al.*, 1996), ACh signalling potency was unaffected by M79A, while Y82A reduced the potency of ACh by 5-fold suggesting that Met79 is not part of the ACh binding site, although Tyr82 may be a “second shell” residue. Again, NDMC responded to these mutations like ACh.

In contrast, M79A significantly reduced the affinity and potency of AC-42 and 77-LH-28-1, while Y82A virtually abolished signalling by both compounds. Y82A also changed the equilibrium interaction between the AC-42 analogues and [<sup>3</sup>H]-NMS from apparently competitive ( $\alpha \leq 0.01$ ) to clearly allosteric ( $\alpha = 0.12, 0.046$  for AC-42, 77-LH-28-1 respectively). The affinities of the selective ligands for the [<sup>3</sup>H]-NMS-occupied receptor were increased at least 5-10-fold by the removal of the Tyr82 side-chain, suggesting that it may help to transmit negatively-cooperative interactions between the ligands.

Interestingly, Tyr82 and Leu102, whose mutation disrupted signalling by the AC-42 analogues, are in contact with the side-chain of Trp101 in molecular models of the M<sub>1</sub> mAChR based either on rhodopsin (Goodwin *et al.*, 2007) or on the  $\beta_2$  adrenergic receptor (Fig 5a). The carboxylate group of Asp105 is 3.6 Å from the indole NH, in the next turn of TM3. Met79 and

Mol #50963

Tyr408 form an extension of this cluster of residues. Leu100, whose mutation is without functional effect, faces the lipid bilayer

How does W101A increase the affinities of AC-42 and 77-LH-28-1? An attractive hypothesis is that deletion of the ring of Trp101 creates a novel binding pocket for a component of AC-42 and 77-LH-28-1. Interestingly, molecular modelling based on the structure of the  $\beta$ -adrenergic receptor suggests that the indole ring of Trp101 can be rotated outwards onto the receptor surface (Fig 5b), potentially opening such a pocket in the wild-type receptor. In the case of 77-LH-28-1, the most likely candidate to occupy the cavity vacated by the Trp indole ring is the dihydroquinolinone side-chain which is similar in size and shape. Anchoring of this moiety may position the protonated nitrogen atom of the adjoining piperidine ring close to the Asp105-Tyr408 duplex, leading to receptor activation by the “back door”. Cys407, whose mutation slightly potentiated the activity of AC-42 and 77-LH-28-1, may form a backstop to the resulting binding site. The proposed site lies within the subsidiary binding pocket between TM2, TM3 and TM7 and is distinct from the “common” allosteric site utilised by prototypical modulators such as gallamine and alcuronium (May *et al.*, 2007).

This model is formalised in the Trp-flip mechanistic scheme shown in Fig.6, in which the equilibrium between the ground and conformationally-isomerised states of the receptor is perturbed by formation of the agonist-receptor complex.

The apparent affinity constant for the agonist is given by

$$K_{app} = K_A \cdot (1 + \beta \cdot K_{Trp}) / (1 + K_{Trp}) \dots \dots \dots (2)$$

Mol #50963

$K_{\text{Trp}}$ , the isomerisation constant, can be calculated from the overall free energy difference in the receptor resulting from the trans to gauche isomerisation of the side-chain of Trp101. This is computed to be  $\sim 3.5$  kcal/mol, yielding a value of  $3 \times 10^{-3}$  for  $K_{\text{Trp}}$ . However, this can be offset by a large value of  $\beta$ , the cooperativity factor describing the ratio of the affinity of the agonist for the isomerised as opposed to the ground state of the receptor. By comparing the estimated free energy contributions of Leu102, and Tyr82 to the binding of the dihydroquinolinone side-chain of 77-LH-28-1 and the indole ring of Trp101 (Table 3), the value of  $\beta$  is roughly estimated to be  $\sim 430$ . The value is assumed to be comparably large for AC-42, but low for ACh and NDMC. The halogenated tricyclic ring system of NDMC may be too bulky to fit the cavity vacated by the indole side-chain, while ligands with less bulky substituents, such as ACh, may be unable to make enough favourable contacts with the surrounding residues to stabilise the conformationally-isomerised state. In the case of the AC-42 analogues, it is solely the complex with the conformationally-isomerised  $R_{\text{W101}^*}$  state that is postulated to have signalling activity.

Generating a pre-formed cavity, as in the W101A mutant, means that the energetic cost (3.5 kcal/mol) of the trans-gauche isomerisation of the side-chain does not have to be paid from the free energy of ligand binding, increasing the effective value of  $K_{\text{Trp}}$  by  $\sim 340$ -fold. For the figures above, which are derived from the indicative energy calculations performed on the  $\beta 2$  adrenergic receptor-based molecular model, a 340-fold increase in  $K_{\text{Trp}}$  enhances  $K_{\text{app}}$  by 96-fold, in good agreement with the experimentally observed effect of the W101A mutation on the affinities of the AC-42 analogues. In principle, the involvement of additional residues neighbouring Trp101 could enhance this value further. In contrast, for the same values, a reduction in the value of  $\beta$ , reflecting the loss of stabilising ligand interactions in the  $R_{\text{W101}^*}$  state



Mol #50963

in the Y82A and L102A mutants, reduces  $K_{app}$  by a maximum of 2.3-fold but could decrease the proportion of  $R_{W101}^*A$  to an arbitrarily low value. In principle, the reduction in  $K_{app}$  can be offset by an increase in  $K_A$ , reflecting the opening up of alternative, but signalling- inactive, binding modes. This may be consistent with the observation of non-competitive binding interactions between the AC-42 analogues and NMS in the Y82A and L102A mutants.

In summary, we suggest a novel conformational trapping mechanism for activation of the  $M_1$  mAChR by AC-42 analogues. The terminal moiety of the side-chain may occupy and stabilise a cavity created by rotation of the side-chain and indole ring of Trp101, positioning the positively-charged ligand nitrogen close to Asp105 in TM3, following a vector distinct from that of ACh. The side-chain rotation may be restricted by sequences elsewhere in the receptor, helping to explain the high functional selectivity of these compounds for the  $M_1$  subtype. Interestingly, Trp often occurs in protein binding sites which undergo large conformational changes on ligand binding (Gunasekaran and Nussinov, 2007). Trp conformational isomerisation may open up novel avenues in drug design. Finally NDMC, like ACh, does not exploit this mechanism.

Mol #50963

## **Acknowledgements**

The authors are grateful to Dr. Alex Goodwin for the construction of the Y82A mutant.

Mol #50963

## Reference List

Baig, A, Leppik, R. A., and Birdsall, N. J. (2005) The Y82A mutant of the M1 receptor has increased affinity and cooperativity with acetylcholine for WIN 62,577 and WIN 51,708. *British Pharmacological Society pA2 online* **31**[2]:119P.

Ballesteros JA and Weinstein H (1995) Integrated Methods for the Construction of Three Dimensional Models and Computational Probing of Structure-Function Relations in G-Protein-Coupled Receptors. *Methods Neurosci* **25**:366-428.

Bee MS and Hulme E C (2007) Functional Analysis of Transmembrane Domain 2 of the M1 Muscarinic Acetylcholine Receptor. *J Biol Chem* **282**:32471-32479.

Blaney FE, Raveglia L F, Artico M, Cavagnera S, Dartois C, Farina C, Grugni M, Gagliardi S, Luttmann M A, Martinelli M, Nadler G M, Parini C, Petrillo P, Sarau H M, Scheideler M A, Hay D W and Giardina G A (2001) Stepwise Modulation of Neurokinin-3 and Neurokinin-2 Receptor Affinity and Selectivity in Quinoline Tachykinin Receptor Antagonists. *J Med Chem* **44**:1675-1689.

Brandish PE, Hill L A, Zheng W and Scolnick E M (2003) Scintillation Proximity Assay of Inositol Phosphates in Cell Extracts: High-Throughput Measurement of G-Protein-Coupled Receptor Activation. *Anal Biochem* **313**:311-318.

Brooks, B. R., Bruccoleri, R. E., Olafson, B. D., States, D. J., Swaminathan, S., and Karplus, M. (1983) CHARMM: A program for macromolecular energy minimization and dynamics calculations. *J Comput Chem* **4**:187-217.

Mol #50963

Cherezov V, Rosenbaum D M, Hanson M A, Rasmussen S G, Thian F S, Kobilka T S, Choi H J, Kuhn P, Weis W I, Kobilka B K and Stevens R C (2007) High-Resolution Crystal Structure of an Engineered Human Beta2-Adrenergic G Protein-Coupled Receptor. *Science* **318**:1258-1265.

Davies MA, Compton-Toth B A, Hufeisen S J, Meltzer H Y and Roth B L (2005) The Highly Efficacious Actions of N-Desmethylozapine at Muscarinic Receptors Are Unique and Not a Common Property of Either Typical or Atypical Antipsychotic Drugs: Is M1 Agonism a Pre-Requisite for Mimicking Clozapine's Actions? *Psychopharmacology (Berl)* **178**:451-460.

de Mendonca FL, da Fonseca P C, Phillips R M, Saldanha J W, Williams T J and Pease J E (2005) Site-Directed Mutagenesis of CC Chemokine Receptor 1 Reveals the Mechanism of Action of UCB 35625, a Small Molecule Chemokine Receptor Antagonist. *J Biol Chem* **280**:4808-4816.

Dunbrack RL and Karplus M (1993) Backbone-Dependent Rotamer Library for Proteins. Application to Side-Chain Prediction. *J Mol Biol* **230**:543-574.

Flanagan CA, Rodic V, Konvicka K, Yuen T, Chi L, Rivier J E, Millar R P, Weinstein H and Sealfon S C (2000) Multiple Interactions of the Asp(2.61(98)) Side Chain of the Gonadotropin-Releasing Hormone Receptor Contribute Differentially to Ligand Interaction. *Biochemistry* **39**:8133-8141.

Goodwin JA, Hulme E C, Langmead C J and Tehan B G (2007) Roof and Floor of the Muscarinic Binding Pocket: Variations in the Binding Modes of Orthosteric Ligands. *Mol Pharmacol* **72**:1484-1496.

Mol #50963

Govaerts C, Bondue A, Springael J Y, Olivella M, Deupi X, Le Poul E, Wodak S J, Parmentier M, Pardo L and Blanpain C (2003) Activation of CCR5 by Chemokines Involves an Aromatic Cluster Between Transmembrane Helices 2 and 3. *J Biol Chem* **278**:1892-1903.

Gunasekaran K and Nussinov R (2007) How Different Are Structurally Flexible and Rigid Binding Sites? Sequence and Structural Features Discriminating Proteins That Do and Do Not Undergo Conformational Change Upon Ligand Binding. *J Mol Biol* **365**:257-273.

Hulme EC, Bee M S and Goodwin J A (2007) Phenotypic Classification of Mutants: a Tool for Understanding Ligand Binding and Activation of Muscarinic Acetylcholine Receptors. *Biochem Soc Trans* **35**:742-745.

Hulme EC, Birdsall N J M and Buckley N J (1990) Muscarinic Receptor Subtypes. *Annu Rev Pharmacol Toxicol* **30**:633-673.

Hulme EC, Lu Z L and Bee M S (2003) Scanning Mutagenesis Studies of the M-1 Muscarinic Acetylcholine Receptor. *Receptors & Channels* **9**:215-228.

Jensen PC, Nygaard R, Thiele S, Elder A, Zhu G, Kolbeck R, Ghosh S, Schwartz T W and Rosenkilde M M (2007) Molecular Interaction of a Potent Nonpeptide Agonist With the Chemokine Receptor CCR8. *Mol Pharmacol* **72**:327-340.

Langmead CJ, Austin N E, Branch C L, Brown J T, Buchanan K A, Davies C H, Forbes I T, Fry V A, Hagan J J, Herdon H J, Jones G A, Jeggo R, Kew J N, Mazzali A, Melarange R, Patel N, Pardoe J, Randall A D, Roberts C, Roopun A, Starr K R, Teriakidis A, Wood M D, Whittington M, Wu Z and Watson J (2008a) Characterization of a CNS Penetrant, Selective M1 Muscarinic Receptor Agonist, 77-LH-28-1. *Br J Pharmacol* **154**:1104-1115.

Mol #50963

Langmead CJ, Fry V A, Forbes I T, Branch C L, Christopoulos A, Wood M D and Herdon H J (2006) Probing the Molecular Mechanism of Interaction Between 4-n-Butyl-1-[4-(2-Methylphenyl)-4-Oxo-1-Butyl]-Piperidine (AC-42) and the Muscarinic M(1) Receptor: Direct Pharmacological Evidence That AC-42 Is an Allosteric Agonist. *Mol Pharmacol* **69**:236-246.

Langmead CJ, Watson J and Reavill C (2008b) Muscarinic Acetylcholine Receptors As CNS Drug Targets. *Pharmacol Ther* **117**:232-243.

Lee SY, Zhu S Z and El-Fakahany E E (1996) Role of Two Highly Conserved Tyrosine Residues in the M1 Muscarinic Receptor Second Transmembrane Domain in Ligand Binding and Receptor Function. *Receptors and Signal Transduction* **6**:43-52.

Leonardi A, Barlocco D, Montesano F, Cignarella G, Motta G, Testa R, Poggese E, Seeber M, De Benedetti P G and Fanelli F (2004) Synthesis, Screening, and Molecular Modeling of New Potent and Selective Antagonists at the Alpha 1d Adrenergic Receptor. *J Med Chem* **47**:1900-1918.

Lu Z-L, Saldanha J and Hulme E C (2001) Transmembrane Domains 4 and 7 of the M<sub>1</sub> Muscarinic Acetylcholine Receptor Are Critical for Ligand Binding and the Receptor Activation Switch. *J Biol Chem* **276**:34098-34104.

Lu Z-L and Hulme E C (1999) The Functional Topography of Transmembrane Domain 3 of the M1 Muscarinic Acetylcholine Receptor, Revealed by Scanning Mutagenesis. *J Biol Chem* **274**:7309-7315.

May LT, Avlani V A, Langmead C J, Herdon H J, Wood M D, Sexton P M and Christopoulos A (2007) Structure-Function Studies of Allosteric Agonism at M2 Muscarinic Acetylcholine Receptors. *Mol Pharmacol* **72**:463-476.

Mol #50963

Page KM, Curtis C A M, Jones P G and Hulme E C (1995) The Functional Role of the Binding Site Aspartate in Muscarinic Acetylcholine Receptors Probed by Site-Directed Mutagenesis. *Eur J Pharmacol* **289**:429-437.

Schetz JA, Benjamin P S and Sibley D R (2000) Nonconserved Residues in the Second Transmembrane-Spanning Domain of the D-4 Dopamine Receptor Are Molecular Determinants of D-4-Selective Pharmacology. *Mol Pharmacol* **57**:144-152.

Simpson MM, Ballesteros J A, Chiappa V, Chen J Y, Suehiro M, Hartman D S, Godel T, Snyder L A, Sakmar T P and Javitch J A (1999) Dopamine D4/D2 Receptor Selectivity Is Determined by a Divergent Aromatic Microdomain Contained Within the Second, Third, and Seventh Membrane-Spanning Segments. *Mol Pharmacol* **56**:1116-1126.

Spalding TA, Ma J N, Ott T R, Friberg M, Bajpai A, Bradley S R, Davis R E, Brann M R and Burstein E S (2006) Structural Requirements of Transmembrane Domain 3 for Activation by the M1 Muscarinic Receptor Agonists AC-42, AC-260584, Clozapine and N-Desmethylozapine: Evidence for Three Distinct Modes of Receptor Activation. *Mol Pharmacol* **70**:1974-1983.

Spalding TA, Trotter C, Skjaerbaek N, Messier T L, Currier E A, Burstein E S, Li D, Hacksell U and Brann M R (2002) Discovery of an Ectopic Activation Site on the M(1) Muscarinic Receptor. *Mol Pharmacol* **61**:1297-1302.

Stitham J, Stojanovic A, Merenick B L, O'Hara K A and Hwa J (2003) The Unique Ligand-Binding Pocket for the Human Prostacyclin Receptor. Site-Directed Mutagenesis and Molecular Modeling. *J Biol Chem* **278**:4250-4257.

Mol #50963

Sur C, Mallorga P J, Wittmann M, Jacobson M A, Pascarella D, Williams J B, Brandish P E, Pettibone D J, Scolnick E M and Conn P J (2003) N-Desmethylozapine, an Allosteric Agonist at Muscarinic 1 Receptor, Potentiates N-Methyl-D-Aspartate Receptor Activity. *Proc Natl Acad Sci U S A* **100**:13674-13679.



Mol #50963

## Footnotes

Guillaume Lebon was supported by a GlaxoSmithKline collaboration award. The work was supported by GlaxoSmithKline and the Medical Research Council (UK).

Reprint requests to: Dr. E.C. Hulme, Division of Physical Biochemistry, MRC National Institute for Medical Research, The Ridgeway, Mill Hill, London NW7 1AA, U.K. Email: ehulme@nimr.mrc.ac.uk

<sup>1</sup> Present address: Division of Structural Studies, Laboratory of Molecular Biology, Hills Road, Cambridge CB2 0QH, U.K.

Mol #50963

## Figure Legends.

**Figure 1:** (a) The structures of agonists used in this study: AC-42, 77-LH-28-1 and NDMC; (b) The locations of the residues mutated.

**Figure 2:** Inhibition by 77-LH-28-1 of specific binding of [<sup>3</sup>H]NMS to membranes prepared from COS-7 cell membranes transfected with wild-type and mutant M<sub>1</sub> mAChRs. Data are the mean ± S.E.M. of quadruplicate measurements obtained using 3 different [<sup>3</sup>H]NMS concentrations (0.1 x, 2 x and 10 x K<sub>d</sub>). Complete data sets were fitted globally to an allosteric ternary complex model of binding giving pK<sub>d</sub> values for [<sup>3</sup>H]NMS and 77-LH-28-1 and cooperativity factors (α) for mutants displaying non-competitive allosteric binding behaviour. Curves show the global fit to the allosteric ternary complex model. **a**, Wild-type; [<sup>3</sup>H]NMS = 0.87 x 10<sup>-9</sup> M (●); 1.7 x 10<sup>-10</sup> M (▼); 1.8 x 10<sup>-11</sup> M (■); pK<sub>d</sub> [<sup>3</sup>H]NMS = 9.74, pK<sub>d</sub> 77-LH-28-1 = 6.54; **b**, W101A; [<sup>3</sup>H]NMS = 3.17 x 10<sup>-9</sup> M (●); 1 x 10<sup>-9</sup> M (▼); 2.1 x 10<sup>-10</sup> M (■); pK<sub>d</sub> [<sup>3</sup>H]NMS = 8.84, pK<sub>d</sub> 77-LH-28-1 = 9.00, α = 0.018 ; **c**, Y82A; [<sup>3</sup>H]NMS = 2.86 x 10<sup>-9</sup> M (●); 5.7 x 10<sup>-10</sup> M (▼); 5.8 x 10<sup>-11</sup> M (■); pK<sub>d</sub> [<sup>3</sup>H]NMS = 9.45, pK<sub>d</sub> 77-LH-28-1 = 6.67, α = 0.046.

**Figure 3:** Mutation-induced changes in the affinities of the antagonist NMS (a) and novel selective agonists NDMC (b), AC-42 (c) and 77-LH-28-1 (d). The histogram represents variations of log affinity constant ΔpK<sub>d</sub> ± SEM for each mutant, compared to the wild type, calculated from Table 1. NC designates non-competitive behaviour, defined by a value of the cooperativity factor α ≥ 0.01 (Materials and Methods). \* P < 0.05, \*\* P < 0.01, \*\*\* P < 0.001 with respect to wild-type.

Mol #50963

**Figure 4:** Representative phosphoinositide dose-response curves showing the action of ACh (●), NDMC (▽), AC-42 (■) and 77-LH-28-1 (◇) on the wild type M<sub>1</sub> mAChR (a) and the following mutants: D105E (b), Y82A (c), L102A (d), Y408F (e) and W101A (f). The receptors were expressed in COS-7 cells labeled with [<sup>3</sup>H]inositol. Phosphoinositide response measurements were carried out using a scintillation proximity assay after 60 min of agonist stimulation. Points represent the mean ± S.E.M. of triplicate determinations. Curves show the fit to a four-parameter logistic function giving values for pEC<sub>50</sub>, E<sub>Max</sub>, E<sub>Basal</sub> and a slope factor (usually about 0.9). E<sub>Max</sub> values were expressed as % of the corresponding value for ACh (Materials and Methods). Values are given as pEC<sub>50</sub> (E<sub>Max</sub>) for ACh (●), NDMC (▽), AC-42 (■) and 77-LH-28-1 (◇) respectively. Values are designated n.d. if they could not be determined. Data shown are typical of three or more independent experiments.

(a) Wild-type: 6.93 (100), 6.37 (42), 5.72 (67), 6.63 (73); (b) D105E: 4.26 (100), n.d., n.d., n.d.; (c) Y82A: 6.20 (100), 6.35 (36), n.d., n.d.; (d) L102A: 4.75 (100), n.d., n.d., 5.40 (36); (e) Y408F: 5.70(100), 6.59 (46), 4.64 (20), 5.33 (42); (f) W101A: 5.49 (100), 6.12 (56), 7.46 (65), 8.70 (56).

**Figure 5:** Model of the M<sub>1</sub> mAChR based on the crystal structure of the β<sub>2</sub> adrenergic receptor. The view is from outside the TM helix bundle. Color coding indicates the effects of the mutations of the residues studied on the potency and maximum signaling response of 77-LH-28-1: Gray, little or no effect; Green, reduced potency; Red, reduced maximum signal; Blue, increased potency. (a) Starting conformation showing the Trp101 side-chain in a trans conformation ( $\chi_1 =$

Mol #50963

167.7°): (b) 77-LH-28-1 (magenta) docked into a binding pocket created by the isomerisation of the side-chain of Trp101 to a gauche<sup>+</sup> conformation ( $\chi_1 = -66^\circ$ ).

**Figure 6:** Trp-flip mechanism showing the equilibrium between the ground state of the receptor ( $R_{W101}$ ) and a state in which the side-chain of Trp101 has undergone conformational isomerisation ( $R_{W101}^*$ ). A represents AC-42 or 77-LH-28-1 and L represents a non-selective orthosteric antagonist, such as NMS. The  $R_{W101}^*A$  state of the receptor is proposed to have signalling activity while the  $R_{W101}A$  state is inactive, in the case of AC-42 and 77-LH-28-1.  $LR_{W101}A$  represents the formation of a (signalling-inactive) ternary complex between the orthosteric antagonist and the NSA.

Mol #50963

**Table 1: Binding affinities of N-methylscopolamine and novel selective agonists for M<sub>1</sub> mAChR mutants.**

Helix	Mutant	Ligand pK <sub>d</sub> (-log M)			
		NMS	NDMC	AC42	77-LH-28-1
	WT	9.86 ± 0.03 <sup>a</sup>	7.41 ± 0.05 <sup>b</sup>	6.14 ± 0.12	6.56 ± 0.08
TM2	M79A	9.52 ± 0.12	7.62 ± 0.06	5.43 ± 0.04**	5.78 ± 0.05**
	Y82A	9.46 ± 0.04	7.15 ± 0.10	6.25 ± 0.10 α = 0.12	6.67 ± 0.20 α = 0.046
TM3	L100A	9.72 ± 0.04	7.20 ± 0.03	5.81 ± 0.02	6.71 ± 0.02
	W101A	8.90 ± 0.03	6.77 ± 0.06**	8.00 ± 0.06***	9.00 ± 0.10*** α = 0.018
	L102A	9.21 ± 0.01	6.58 ± 0.04**	6.52 ± 0.04** α = 0.046	6.61 ± 0.05 α = 0.01
	D105E	9.47 ± 0.02	7.04 ± 0.08*	5.86 ± 0.05	6.7 ± 0.05
TM7	Y404A	8.11 ± 0.04	7.01 ± 0.03** α = 0.046	6.03 ± 0.03	6.58 ± 0.03
	Y404F	8.80 ± 0.008	7.57 ± 0.04	5.89 ± 0.04	6.43 ± 0.05
	C407A	8.31 ± 0.04	6.92 ± 0.03**	5.74 ± 0.05*	6.29 ± 0.03
	Y408A	8.04 ± 0.03	7.85 ± 0.07**	6.37 ± 0.03	6.37 ± 0.03
	Y408F	8.98 ± 0.03	7.49 ± 0.05	5.41 ± 0.04 **	5.67 ± 0.03***

The affinity constants pK<sub>d</sub> (- log M) for [<sup>3</sup>H]NMS, NDMC, AC-42 and 77-LH-28-1, are tabulated. A cooperativity factor value α is specified where its inclusion significantly improved the global fit to an allosteric ternary complex model of ligand-[<sup>3</sup>H]NMS interaction (see Materials and Methods). Otherwise the interactions appeared competitive. <sup>a</sup>pK<sub>d,NMS</sub> values were estimated using three different NMS concentrations, equivalent to 0.1 x, 2 x and 10 x K<sub>d</sub>; values are the means of 5 different experiments for each mutant ± SEM. <sup>b</sup>Values are the mean ± SEM of measurements using 3 different [<sup>3</sup>H]NMS concentrations (0.1 x, 2 x and 10 x K<sub>d</sub>): Slope factors of binding curves were close to 1.0. \* P<0.05, \*\* P<0.01, \*\*\* P<0.001 significantly different to wild type receptor.

Mol #50963

**Table 2: Phosphoinositide responses evoked by the action of ACh and novel selective agonists on M<sub>1</sub> mAChR mutants.**

Helix	Mutant	ACh	NDMC		AC-42		77-LH-28-1	
		pEC <sub>50</sub>	pEC <sub>50</sub>	E <sub>MaxN</sub>	pEC <sub>50</sub>	E <sub>MaxN</sub>	pEC <sub>50</sub>	E <sub>MaxN</sub>
	WT	6.92 ± 0.04	6.42 ± 0.05	52.2 ± 7.0	5.79 ± 0.03	64.3 ± 2.7	6.68 ± 0.08	74.0 ± 0.4
TM2	M79A	6.73 ± 0.18	6.00 ± 0.06	40.7 ± 6.5	5.29 ± 0.05 *	55.6 ± 8.0	6.14 ± 0.11 *	81.3 ± 8.3
	Y82A	6.25 ± 0.07 *	6.16 ± 0.10	44.2 ± 5.0	n.d.	n.d.	n.d.	n.d.
TM3	L100A	6.78 ± 0.14	6.04 ± 0.20	35.2 ± 2.7	5.52 ± 0.02	56.8 ± 3.9	6.58 ± 0.03	66.6 ± 4.1
	W101A	5.38 ± 0.08 ***	6.17 ± 0.03	54.7 ± 3.6	7.57 ± 0.09 ***	70.8 ± 5.6	8.72 ± 0.02 ***	59.9 ± 10.1
	L102A	4.81 ± 0.03 ***	n.d. <sup>a</sup>	n.d.	n.d.	n.d.	5.41 ± 0.11 ***	30.0 ± 1.9 **
	D105E	4.20 ± 0.03 ***	n.d.	0	n.d.	0	n.d.	0
TM7	Y404A	4.58 ± 0.16 ***	6.42 ± 0.28	58.3 ± 3.9	6.07 ± 0.16	70.8 ± 13.9	7.07 ± 0.18	83.6 ± 11.3
	Y404F	4.88 ± 0.25 ***	6.37 ± 0.07	21.5 ± 4.6 **	5.81 ± 0.17	68.4 ± 4.6	6.92 ± 0.23	75.4 ± 3.6
	C407A	5.51 ± 0.07 ***	5.80 ± 0.04 *	29.7 ± 4.3 **	5.69 ± 0.05	80.1 ± 25.0	6.53 ± 0.05	104.1 ± 32
	Y408A	5.11 ± 0.16 ***	6.98 ± 0.18 *	34.0 ± 4.4	4.61 ± 0.10 ***	21.4 ± 6.2 *	6.01 ± 0.10 **	34.0 ± 9.1
	Y408F	5.34 ± 0.28 ***	6.74 ± 0.08	45.3 ± 5.1	4.93 ± 0.30 **	24.3 ± 2.2 *	5.26 ± 0.06 ***	44.6 ± 3.7

Compound dilutions were added in triplicate in Krebs-Li solution. An equivalent concentration of DMSO (1 %) was present in all incubations. In each experiment, atropine (10<sup>-6</sup> M) was added to one triplicate set of assays to control for atropine-sensitive ACh-independent constitutive activity. This was maximally 8.5 % for the wild-type receptor. Dose-response curves were fitted to a four-parameter logistic function, yielding E<sub>Max</sub>, E<sub>Basal</sub>, and pEC<sub>50</sub> values for each NSA at the particular mutant under study. E<sub>Max</sub> values for the NSAs, corrected for basal signaling, were expressed relative to the corresponding values for ACh in the same experiment as follows  $E_{MaxN} = (E_{MaxNSA} - E_{Basal}) / (E_{MaxACh} - E_{Basal})$ . The value taken for E<sub>Basal</sub> was the measurement conducted in the presence of atropine, except in the case of L102A, D105E and Y404A where the values were not different. pEC<sub>50</sub> and E<sub>MaxN</sub> values are tabulated. The values are mean ± SEM of 3-4

Mol #50963

separate measurements. \*  $P < 0.05$ , \*\*  $P < 0.01$ , \*\*\*  $P < 0.001$  significantly different to wild-type receptor; <sup>a</sup> n.d. response too low to quantify.

Mol #50963

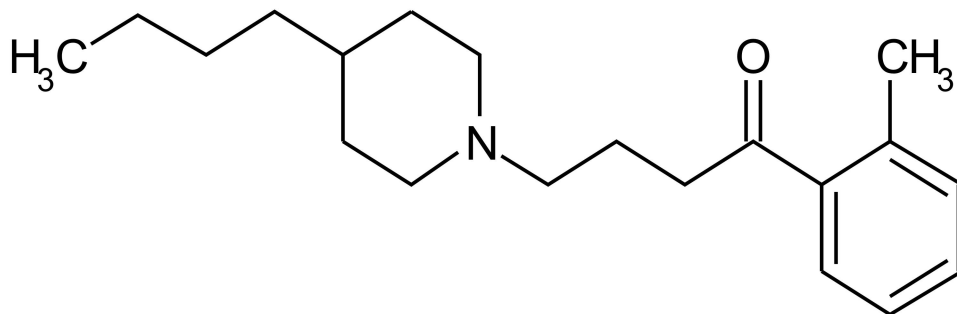
**Table 3: Computed interaction energies of the indole side-chain of W101, and of the ligand 77-LH-28-1 calculated using a structural model of the M<sub>1</sub> mAChR.**

Residue	Trp 101 indole ring <sup>a</sup> (kcal/mol)			77-LH-28-1 <sup>b</sup> (kcal/mol)		
	electronic	steric	total	electronic	steric	total
<b>TYR 82</b>	0.064 <sup>c</sup>	-2.246	-2.181	-0.131	-5.839	-5.969
<b>LEU 102</b>	-0.022	-2.827	-2.849	-0.073	-2.632	-2.706

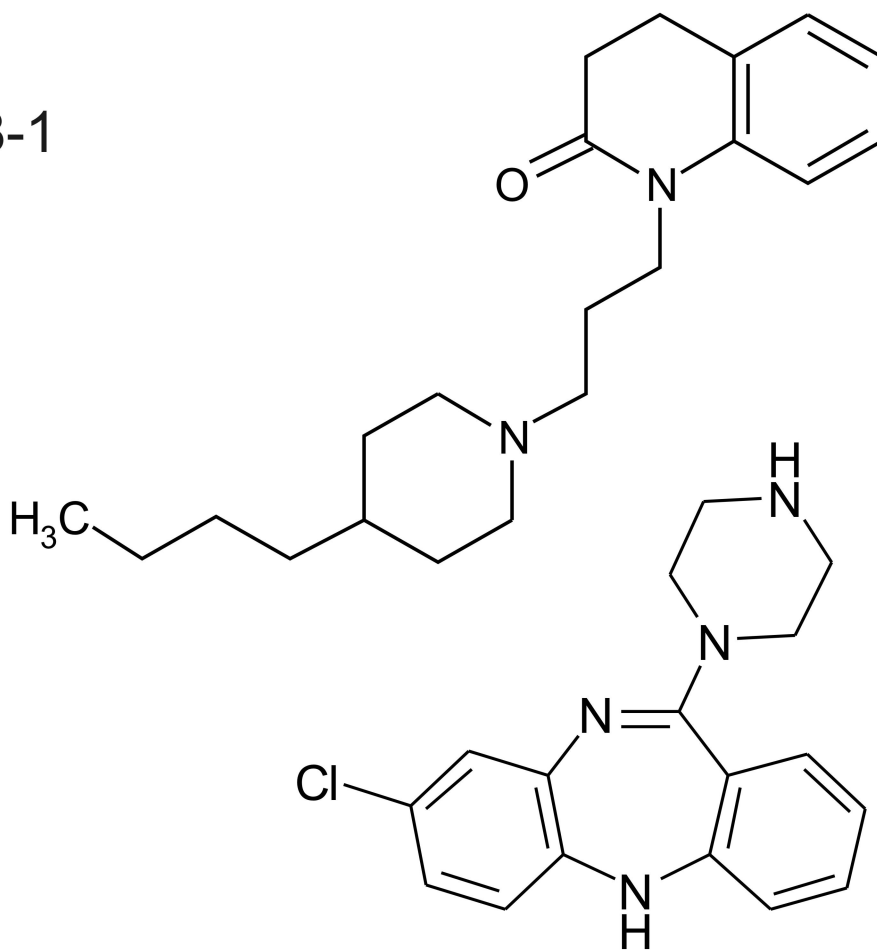
A homology model of the M<sub>1</sub> mAChR was constructed on the structure of the β<sub>2</sub> adrenergic receptor and optimised (Materials and Methods). <sup>a</sup>Interaction energies for the indole side-chain of Trp101 with the side-chains of Tyr82 and Leu102 were calculated by energy deconvolution using a trans conformation ( $\chi_1 = 167.7^\circ$ ) of the Trp101 side-chain. <sup>b</sup>Following rotation of the side-chain of Trp101 to give  $\chi_1 = -60^\circ$  (gauche<sup>+</sup> conformation), 77-LH-28-1 was docked into the resulting binding pocket and the resulting structure subjected to final energy minimisation resulting in a  $\chi_1$  angle of  $-66^\circ$  for Trp101. The interaction energies of the atoms of 77-LH-28-1 with Tyr82 and Leu102 were then calculated by energy deconvolution (Materials and Methods). <sup>c</sup> Values are the sum of the calculated interaction energies between the indicated moieties, kcal/mol.



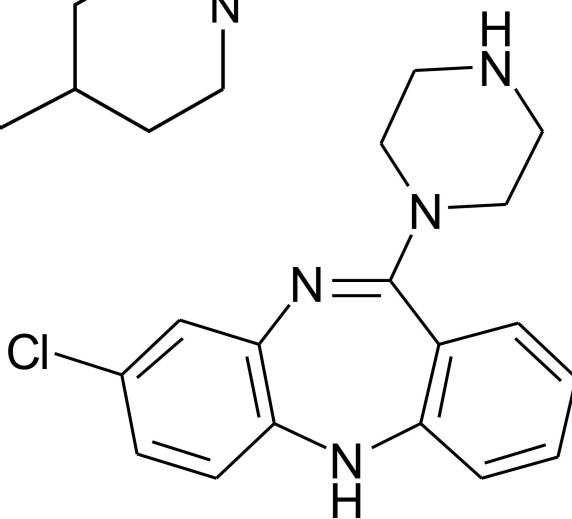
AC-42



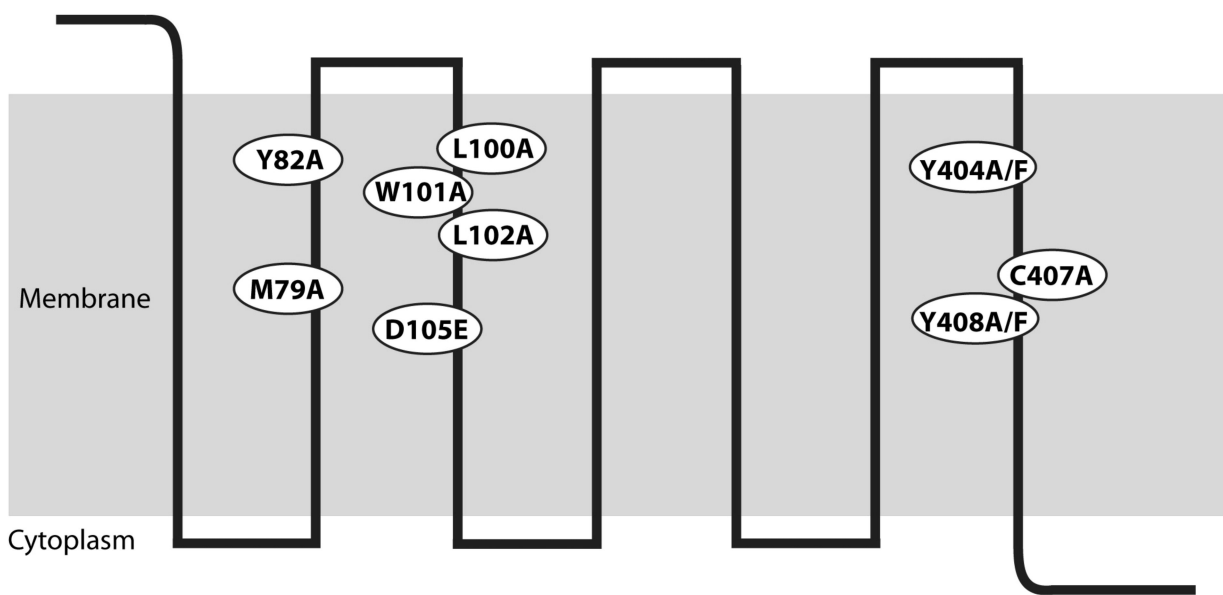
77-LH-28-1



NDMC



(a)



(b)

Figure 2.

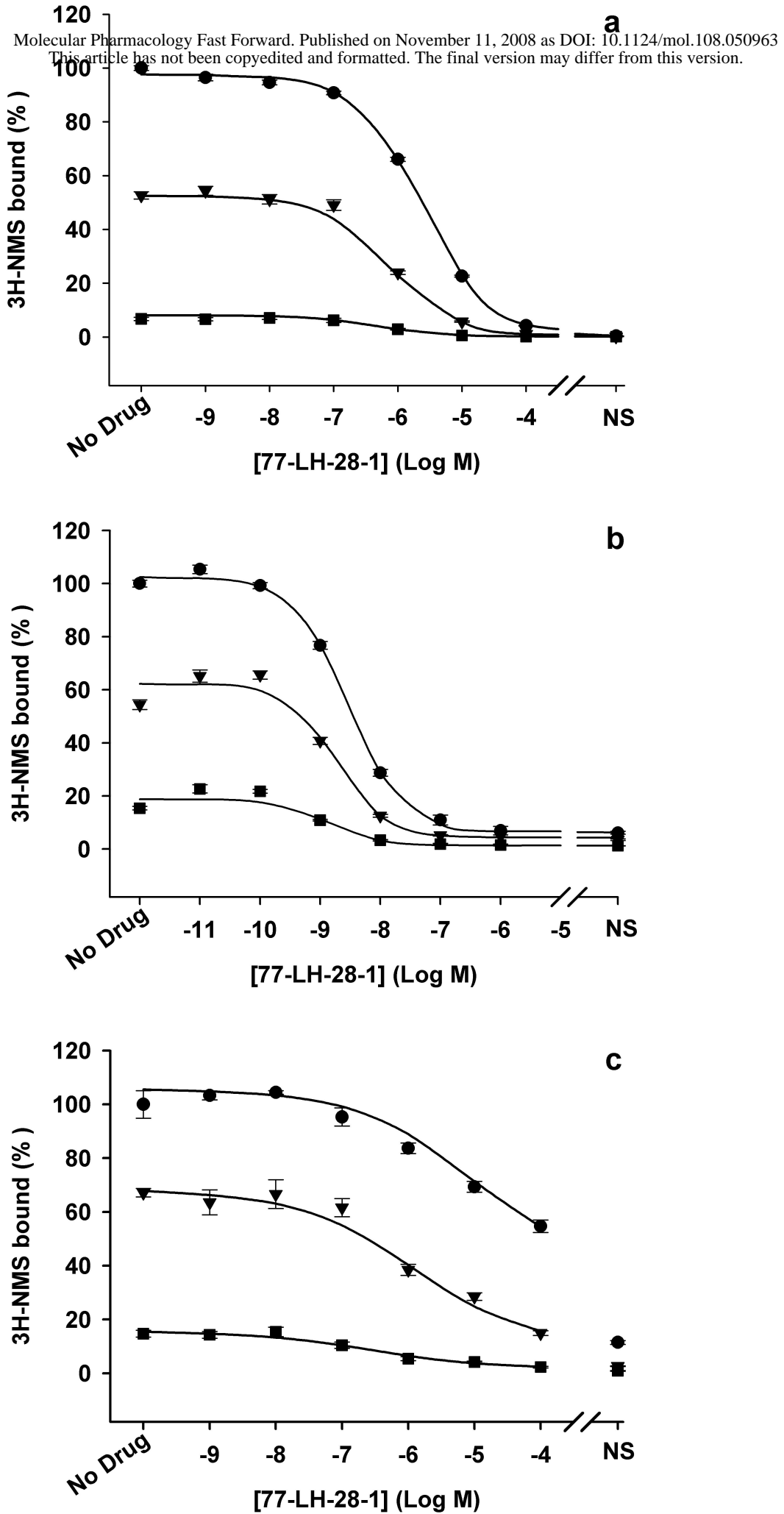


**Figure 3.**

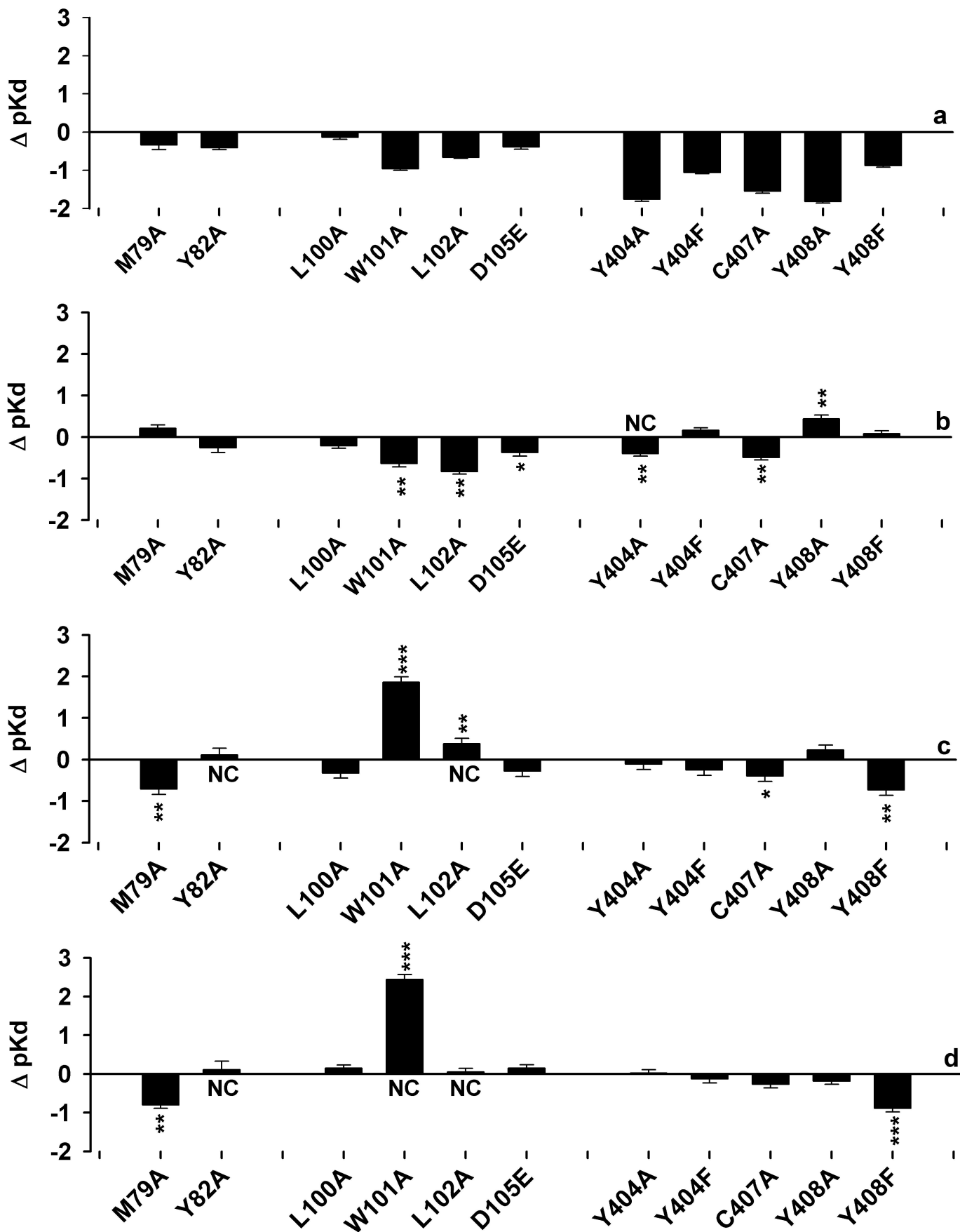


# Figure 4.

Molecular Pharmacology Fast Forward. Published on November 11, 2008 as DOI: 10.1124/mol.108.050963  
This article has not been copyedited and formatted. The final version may differ from this version.

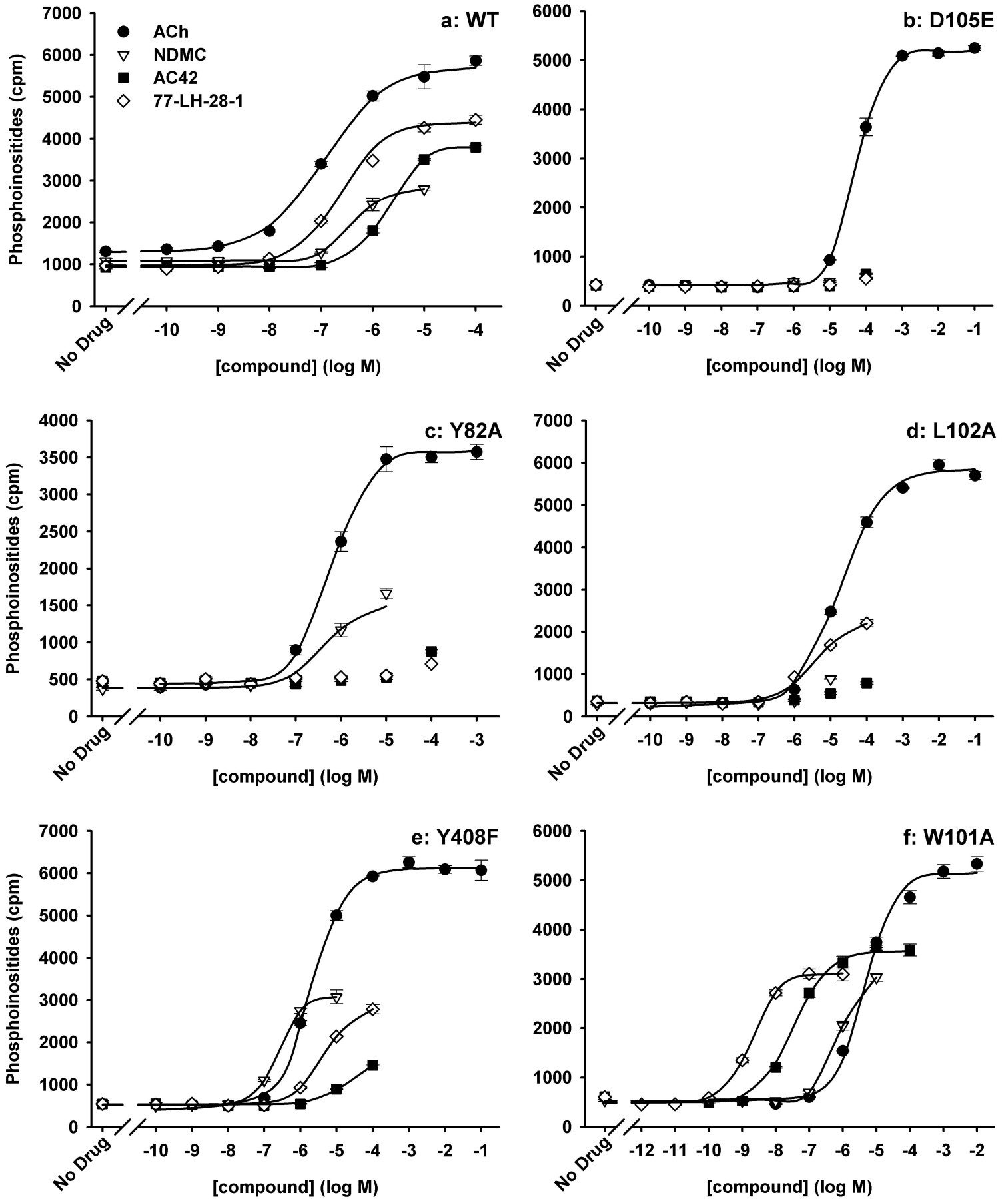


**Figure 5.**

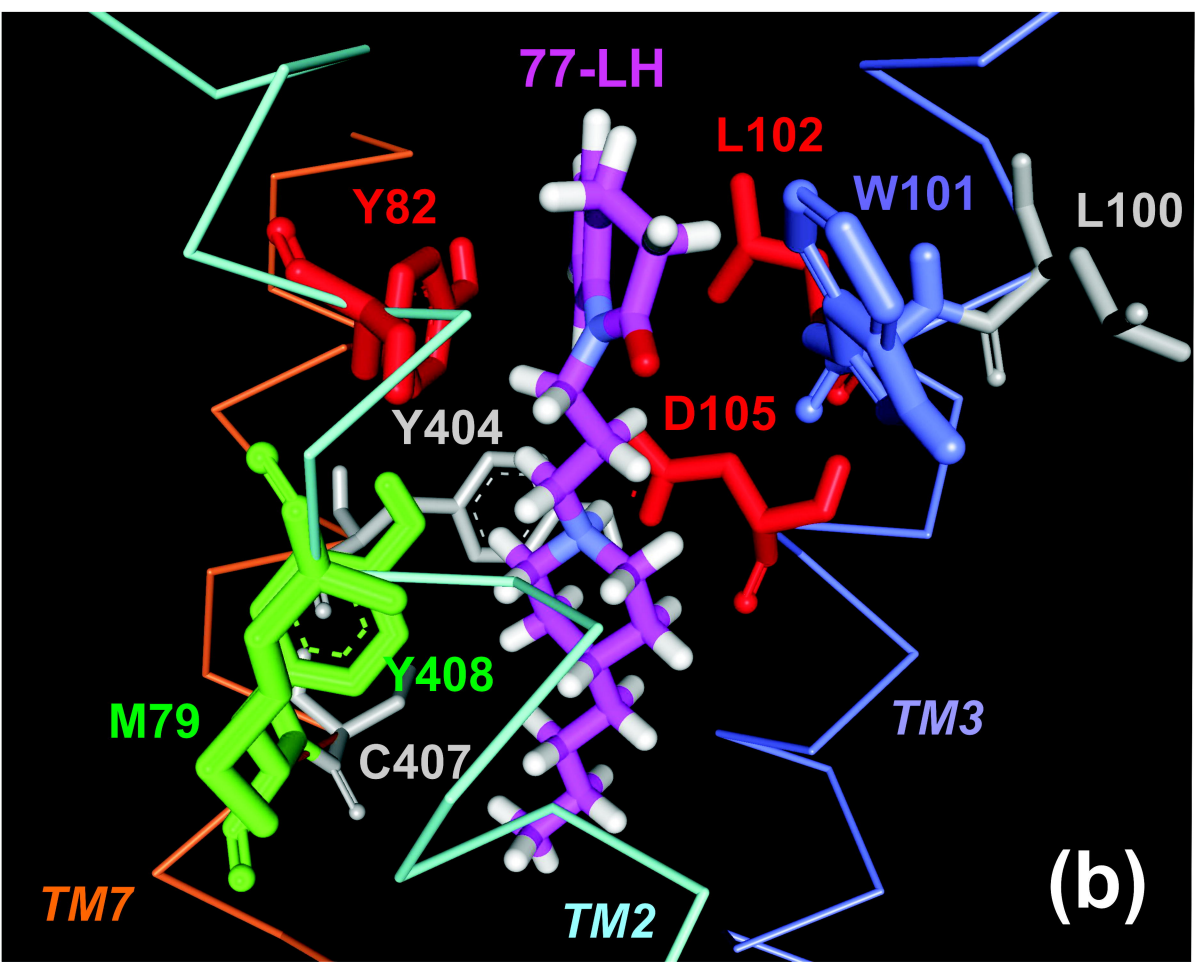
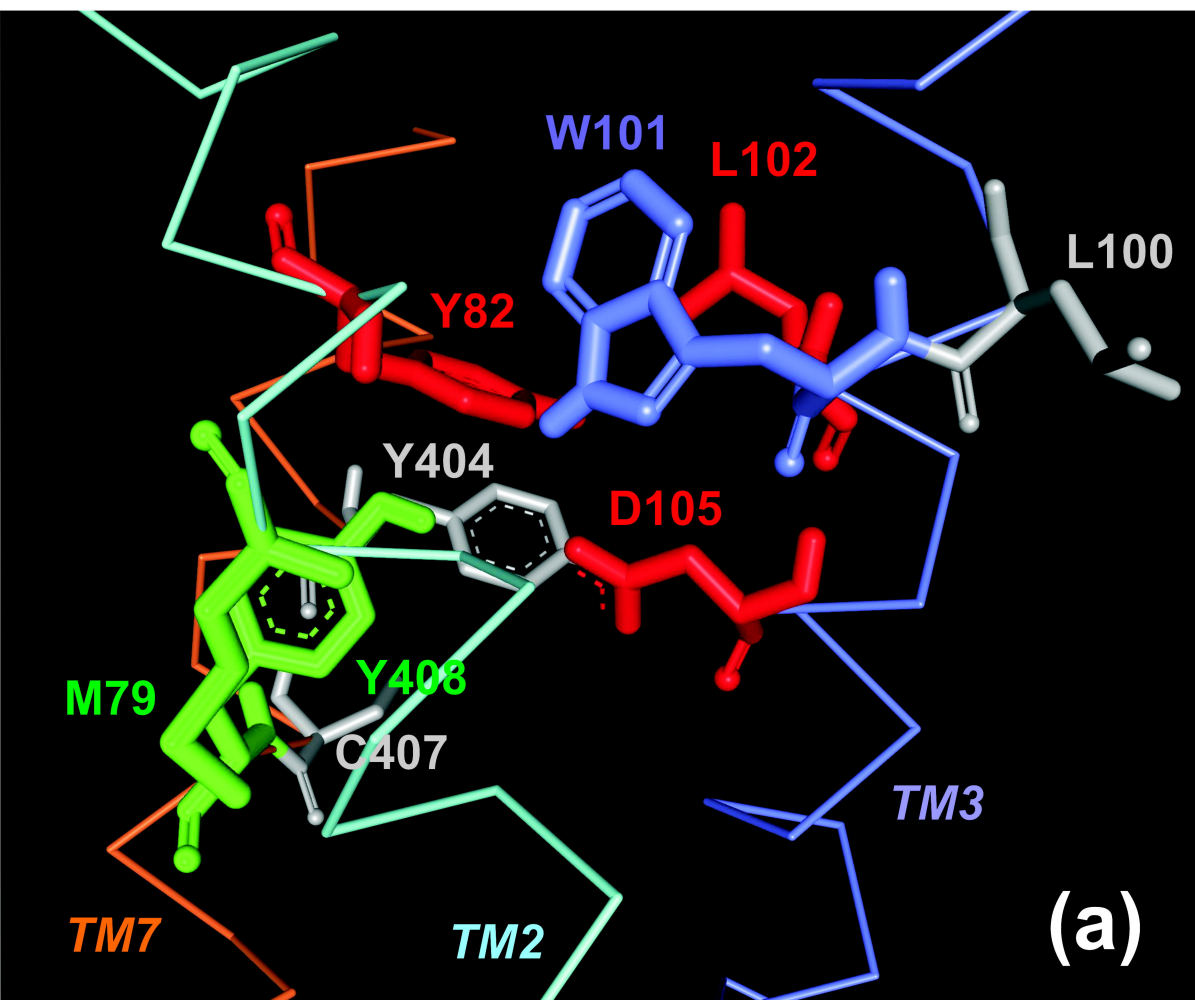


Figure 6.

